

## Supporting Information

### **An implantable and versatile piezoresistive sensor for the monitoring of human-machine interfacing interactions and dynamical process of nerve repair**

Ping Wu<sup>a</sup>, Ao Xiao<sup>a</sup>, Yanan Zhao<sup>a</sup>, Feixiang Chen<sup>a</sup>, Meifang Ke<sup>a</sup>, Qiang Zhang<sup>a</sup>,  
Jianwei Zhang<sup>b</sup>, Xiaowen Shi<sup>b</sup>, Xiaohua He<sup>a</sup> and Yun Chen<sup>a, c\*</sup>

<sup>a</sup> Department of Biomedical Engineering, School of Basic Medical Sciences, Wuhan University, Wuhan 430071, China

<sup>b</sup> School of Resource and Environmental Science, Hubei International Scientific and Technological Cooperation Base of Sustainable Resource and Energy, Wuhan University, Wuhan 430079, China

<sup>c</sup> Hubei Province Key Laboratory of Allergy and Immune Related Diseases, Wuhan University, Wuhan 430071, China

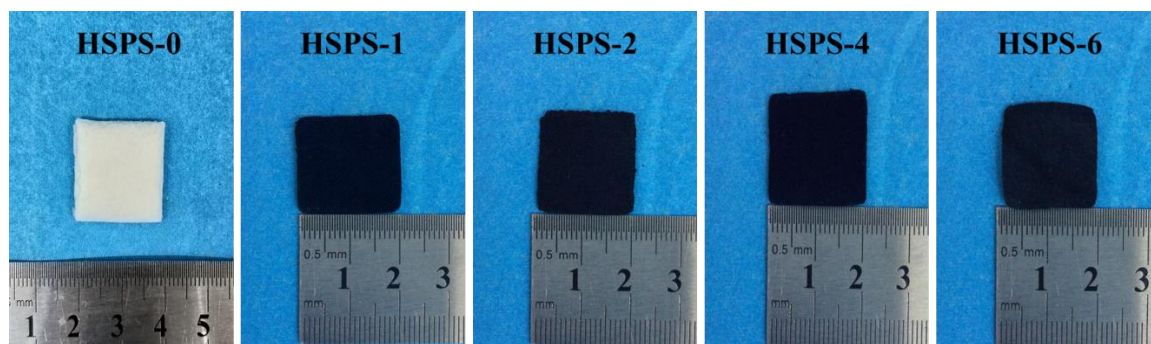


Figure S1. Photograph of HSPS-*t*

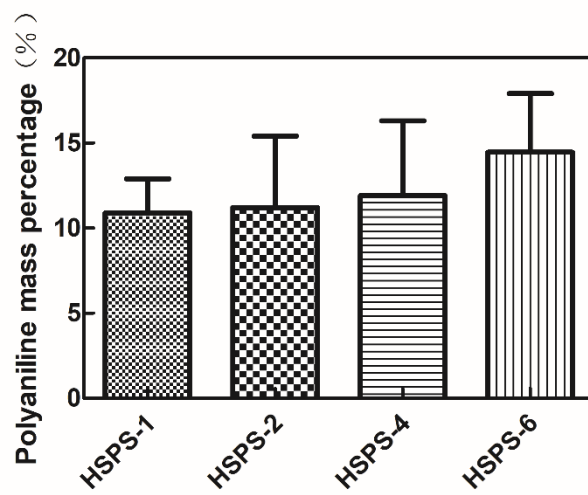


Figure S2. Polyaniline mass percentage in HSPS-1, HSPS-2, HSPS-4 and HSPS-6

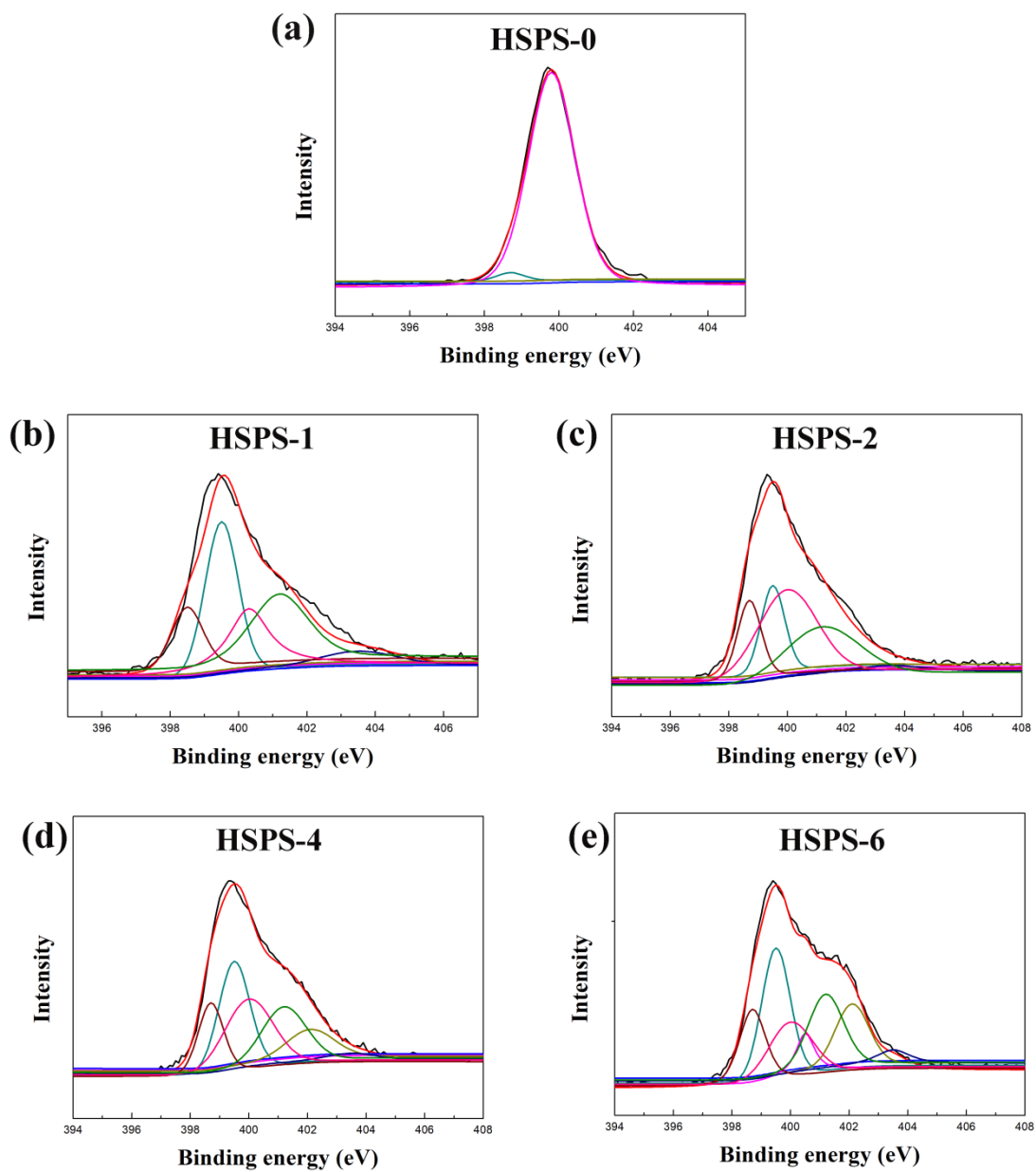


Figure S3.  $N_{1s}$  core level spectra of HSPS- $t$

Table S1. XPS results of HSPS-*t*

		- N=	- N -	- N <sup>+</sup>	=N <sup>+</sup>	NH/N-C	C=N/N-C	H-N-COO/ N-C=C (SPI)
		(PANI)	(PANI)	(PANI)	(PANI)	(SPI)	(SPI)	(SPI)
<b>HSPS-0</b>	Binding energy (eV)	399.5	400.5	402.5	403.5	398.7	399.8	401.2
	Binding area (%)	-	-	-	-	3.3	96.7	≈0
<b>HSPS-1</b>	Binding energy (eV)	399.5	400.5	402.5	403.5	398.5	400	401.2
	Binding area (%)	33.3	≈0	≈0	6.7	7.7	23.6	28.7
<b>HSPS-2</b>	Binding energy(eV)	399.5	400.5	402.5	403.5	398.7	400	401.2
	Binding area (%)	15.7	≈0	0.7	2.9	15.6	38.7	26.4
<b>HSPS-4</b>	Binding energy(eV)	399.5	400.5	402.5	403.5	398.5	400	401.2
	Binding area (%)	26.7	≈0	10.6	2.2	15.6	25.9	19
<b>HSPS-6</b>	Binding energy(eV)	399.5	400.5	402.5	403.5	398.5	400	401.2
	Binding area (%)	25	7.6	13.8	4.2	15.6	15.7	18.1

Table S2. The  $(-N^+ + =N^+)/N$  percentage in PANI of HSPS-1, HSPS-2, HSPS-3 and HSPS-4

	HSPS-1	HSPS-2	HSPS-4	HSPS-6
$(-N^+ + =N^+)/N$ percentage (%)	16.7	18.5	32.4	35.6

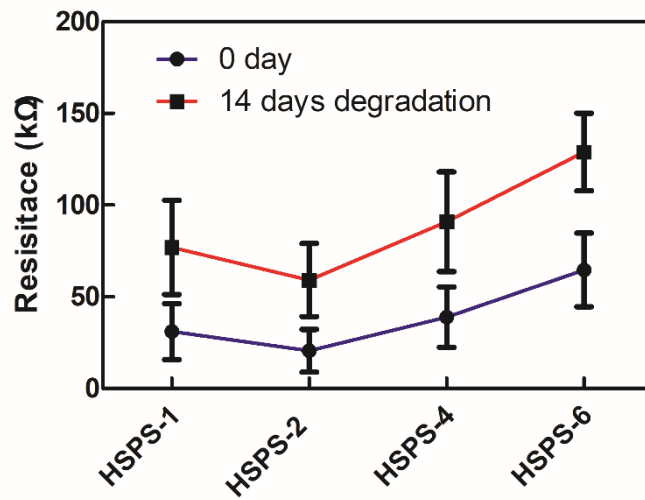


Figure S4. The resistance of HSPS-1, HSPS-2, HSPS-4 and HSPS-6 after 0 and 14 days of *in vitro* degradation

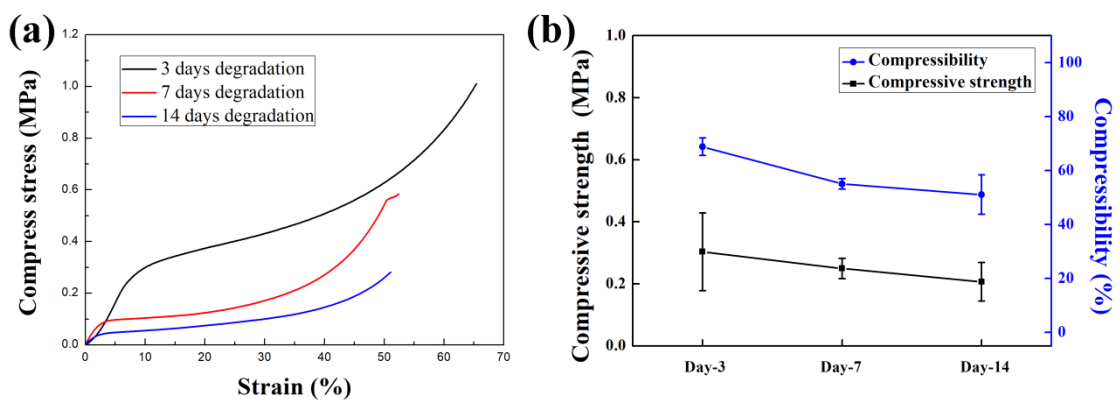


Figure S5. The compressive stress-strain (a), compressibility and compressive strength curves (b) of the HSPS-2 sponge after 3, 7 and 14 days *in vitro* degradation

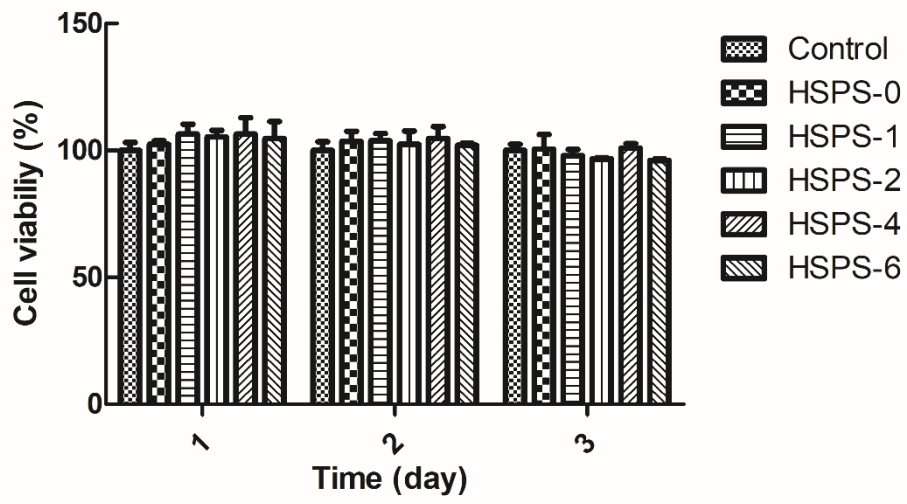


Figure S6. Cell viability of L929 cells incubated with HSPS-*t* extract

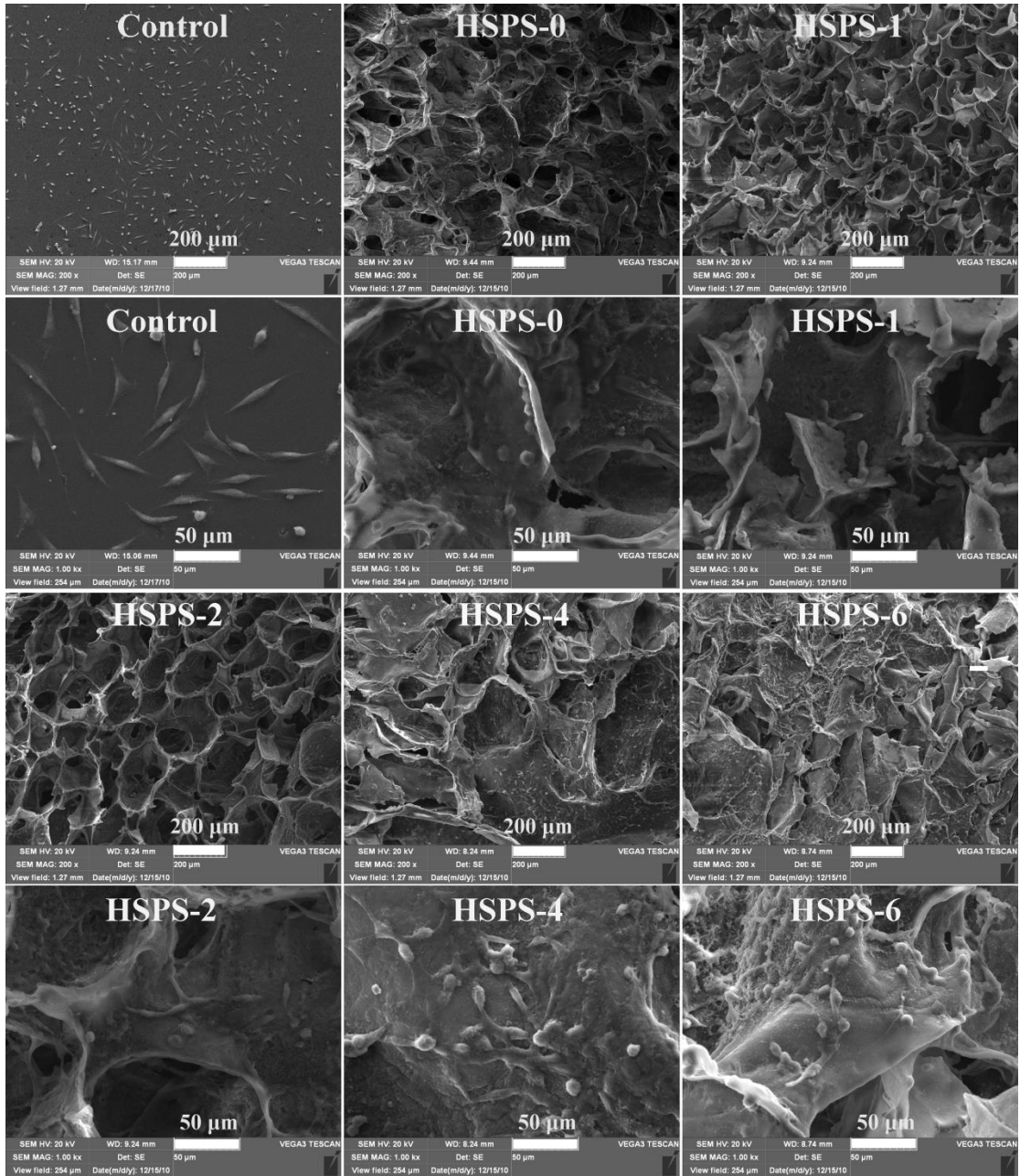


Figure S7. SEM images of L929 cells cultured on tissue culture plate (control) and the surface of HSPS-*t*.



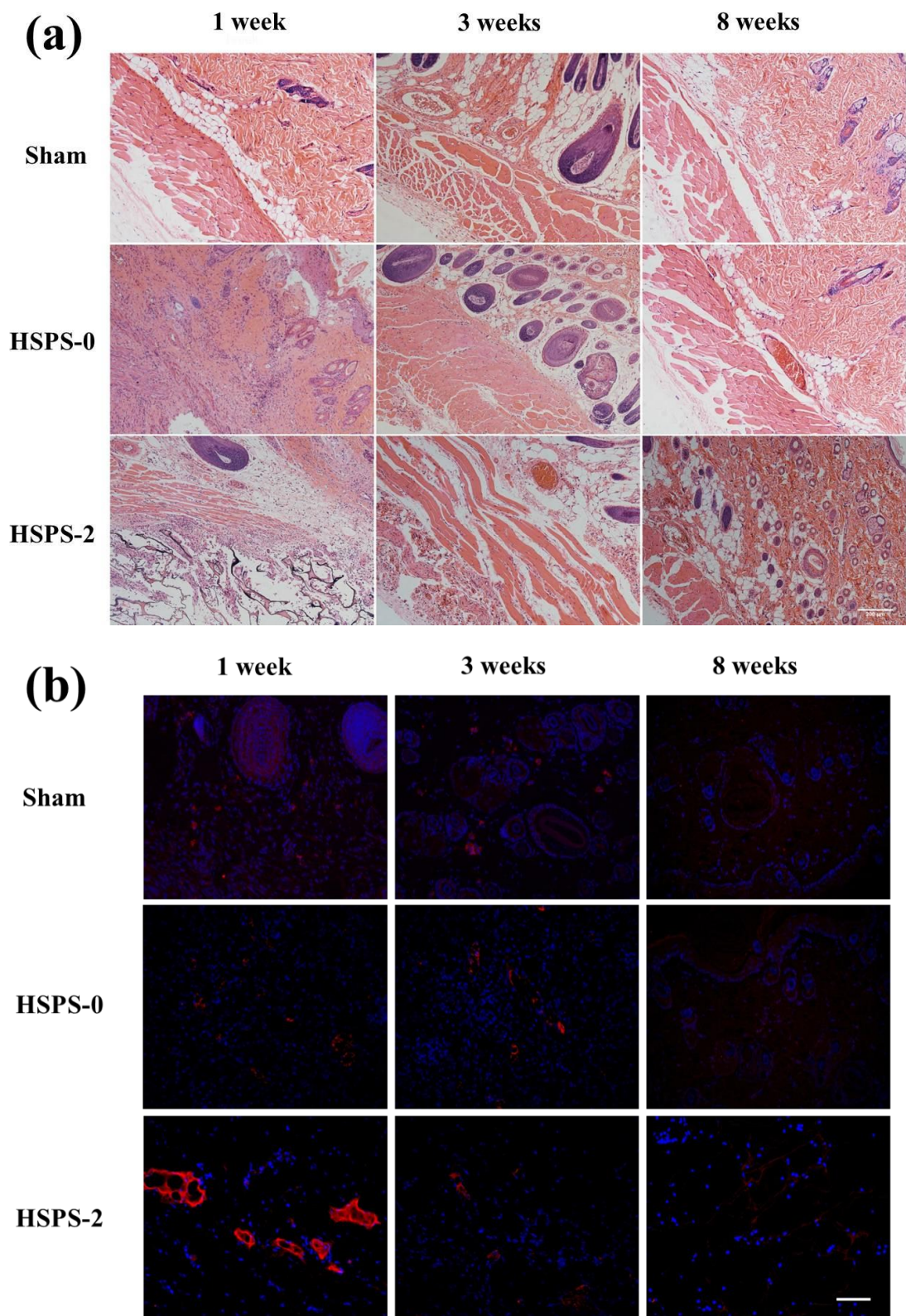


Figure S8. Biocompatibility of sham-operation, HSPS-0 and HSPS-2 sponges evaluated *in vivo*. (a) HE-staining after sensor implantation, scar bar=200  $\mu\text{m}$ , (b) Immunofluorescent-staining after sensor implantation, scale bar=50  $\mu\text{m}$ .



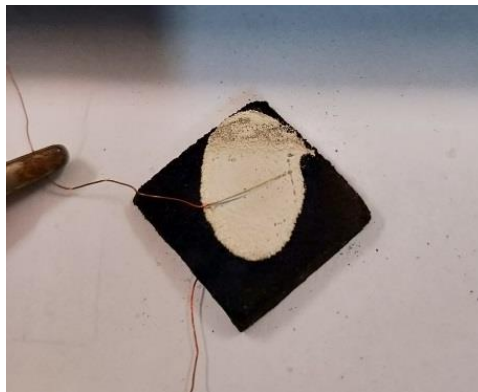


Figure S9. HSPS-2 sponge coated with conductive silver paste